JVI Journals.ASM.org

Characterization of pH-Sensitive Molecular Switches That Trigger the Structural Transition of Vesicular Stomatitis Virus Glycoprotein from the Postfusion State toward the Prefusion State

Anna Ferlin, Hélène Raux, Eduard Baquero, Jean Lepault, Yves Gaudin

Centre de Recherche de Gif, Laboratoire de Virologie Moléculaire et Structurale, CNRS (UPR 3296), Gif sur Yvette, France

ABSTRACT

Vesicular stomatitis virus (VSV; the prototype rhabdovirus) fusion is triggered at low pH and mediated by glycoprotein G, which undergoes a low-pH-induced structural transition. A unique feature of rhabdovirus G is that its conformational change is reversible. This allows G to recover its native prefusion state at the viral surface after its transport through the acidic Golgi compartments. The crystal structures of G pre- and postfusion states have been elucidated, leading to the identification of several acidic amino acid residues, clustered in the postfusion trimer, as potential pH-sensitive switches controlling the transition back toward the prefusion state. We mutated these residues and produced a panel of single and double mutants whose fusion properties, conformational change characteristics, and ability to pseudotype a virus lacking the glycoprotein gene were assayed. Some of these mutations were also introduced in the genome of recombinant viruses which were further characterized. We show that D268, located in the segment consisting of residues 264 to 273, which refolds into postfusion helix F during G structural transition, is the major pH sensor while D274, D395, and D393 have additional contributions. Furthermore, a single passage of recombinant virus bearing the mutation D268L (which was demonstrated to stabilize the G postfusion state) resulted in a pseudorevertant with a compensatory second mutation, L271P. This revealed that the propensity of the segment of residues 264 to 273 to refold into helix F has to be finely tuned since either an increase (mutation D268L alone) or a decrease (mutation L271P alone) of this propensity is detrimental to the virus.

IMPORTANCE

Vesicular stomatitis virus enters cells via endocytosis. Endosome acidification induces a structural transition of its unique glycoprotein (G), which mediates fusion between viral and endosomal membranes. G conformational change is reversible upon increases in pH. This allows G to recover its native prefusion state at the viral surface after its transport through the acidic Golgi compartments. We mutated five acidic residues, proposed to be pH-sensitive switches controlling the structural transition back toward the prefusion state. Our results indicate that residue D268 is the major pH sensor, while other acidic residues have additional contributions, and reveal that the propensity of the segment consisting of residues 264 to 273 to adopt a helical conformation is finely regulated. This segment might be a good target for antiviral compounds.

The entry of enveloped viruses into cells requires the fusion of viral and cellular membranes. This process is mediated by viral glycoproteins that, upon interactions with specific triggers (e.g., low-pH environment or cellular receptors), undergo conformational changes that drive fusion. These structural rearrangements result in the exposure of hydrophobic motifs (the so-called fusion peptides or fusion loops), which then interact with one or both of the participating membranes, resulting in their destabilization and merger. Several classes of fusion glycoproteins have been identified based on common structural motifs (1–3).

Regardless of the class of the fusion glycoprotein, triggering the conformational change in the absence of a target membrane leads to inactivation of the fusion properties (4). Therefore, premature activation has to be precluded. More specifically, during the maturation and transport of fusion glycoproteins through the Golgi apparatus, they encounter acidic compartments (5). It appears that viruses for which fusion is triggered at low pH have the ability to protect their fusion proteins from the deleterious acidic environment of the Golgi apparatus. Indeed, for influenza virus, the pH of the transport vesicles is regulated by the virally encoded M2 protein (6), which is a proton channel (7). Furthermore, the cleavage of the native hemagglutinin (HA0) into HA1 and HA2, which is absolutely required for the low-pH-induced conformational change, occurs at a late stage of transport (8) or even after viral budding in the extracellular medium (9). Similarly, class II fusion proteins are transported in association with a viral chaperone protein. In this complex, the fusion glycoprotein is protected from premature activation. The cleavage of this accompanying protein, which is required for promoting viral fusion under biological conditions, takes place only after transport through the Golgi apparatus (10, 11).

The *Rhabdoviridae* are enveloped bullet-shaped viruses that are widespread among a great variety of organisms, including plants, insects, crustaceans, fishes, reptiles, and mammals (12).

Received 9 July 2014 **Accepted** 2 September 2014
Published ahead of print 10 September 2014
Editor: D. S. Lyles
Address correspondence to Yves Gaudin, gaudin@vms.cnrs-gif.fr.
A.F. and H.R. contributed equally to this article.

doi:10.1128/JVI.01962-14

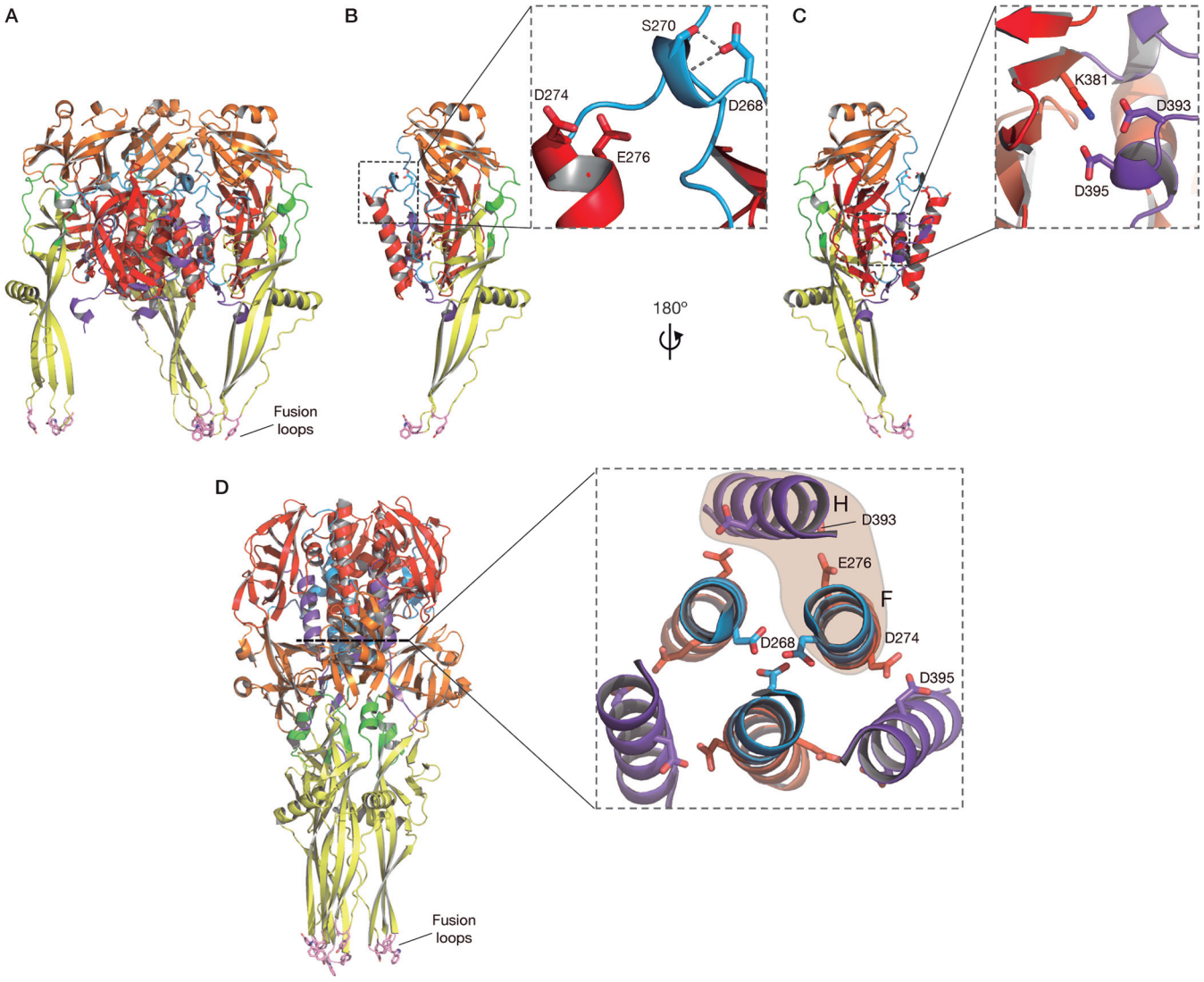

FIG 1 Ribbon representation of the structure of VSV glycoprotein showing the position of the residues which have been mutated in this work. (A) Prefusion trimer. (B and C) Prefusion protomer. (D) Postfusion trimer. The protein domains are represented as follows: yellow, fusion domain (FD); red, the central trimerization domain (TrD); orange, pleckstrin homology domain (PHD). The segments connecting FD to PHD are shown in green, those connecting PHD to TrD are in cyan, and the C-terminal segment is in magenta. Residues in the fusion loops are in stick representation and shown in pink. The inset in panel B is an enlargement of residues D268, D274, and E276. In its deprotonated form, the lateral chain of D268 is involved in two hydrogen bonds with S270 (with the OH group of the lateral chain and the NH group of the peptide bond). The inset in panel C is an enlargement of residues D393 and D395 which make salt bridges with K381. The inset in panel D is a bottom view of the central six-helix bundle of the postfusion conformation. In this inset, helices H and F belonging to the same protomer are indicated.

This family includes vesicular stomatitis virus (VSV), the prototype of the *Vesiculovirus* genus, as well as rabies virus (RABV), the prototype of the *Lyssavirus* genus. In their membranes, rhabdoviruses have a single glycoprotein (G) that mediates both virus attachment to specific receptors and, after virion endocytosis, fusion between viral and endosomal membranes (13). For both RABV and VSV, it has been demonstrated that low-pH-induced structural transition of G is reversible (14, 15). In fact, at the viral surface, there is a pH-dependent thermodynamic equilibrium between different states of G, which is shifted toward the trimeric postfusion form at low pH (16–18). This is the main difference between rhabdoviral G and other viral fusion glycoproteins activated at low pH for which the prefusion conformation is metastable and, as a consequence, the low-pH-induced structural transition is irreversible (4). The reversibility of its conformational change allows G to be transported through the acidic compartment of the Golgi apparatus and to recover its native prefusion state at the viral surface (19).

VSV G is the only class III fusion protein for which the trimeric structures of both the pre- and postfusion states of a soluble form of the ectodomain have been determined (20, 21) (Fig. 1). The polypeptide chain of the G ectodomain folds into three distinct domains. The fusion domain (FD) is made of an extended β-sheet structure at the tip of which are located two loops that constitute the membrane-interacting motif of the G ectodomain (22, 23). FD is inserted in a loop of a pleckstrin homology domain (PHD) that

is itself inserted into a central domain (TrD) which is involved in trimerization of the molecule in both the pre- and postfusion states. These rigid domains are connected by segments which undergo major refolding events during the structural change (24). Particularly, during the transition to the postfusion state, the central helix is lengthened by the recruitment of the segment made up of residues 263 to 275 to form the long helix F, and residues 384 to 400 refold into helix H. Helix H positions itself in the grooves of the central core made of helix F in an antiparallel manner to form the central six-helix bundle of the postfusion conformation (20).

Several acidic residues (D268, D274, E276, D393, and D395) are brought close together in the postfusion six-helix bundle. It has been suggested that these residues play the role of pH-sensitive molecular switches as, in their deprotonated forms, they should destabilize the central six-helix bundle (Fig. 1) and thus allow the refolding of G back toward its prefusion conformation (21).

In this work, we have mutated these acidic residues by the corresponding amide residue (i.e., Asp by Asn and Glu by Gln) or, in the case of Asp 268, by hydrophobic Leu. Several mutants were affected in their fusion properties and do not efficiently pseudotype a virus lacking the glycoprotein gene. Characterization of the pH-dependent stability of the postfusion conformation of mutant glycoproteins identified D268 as a major pH-sensitive switch. Finally, when the corresponding mutations were introduced in the genome of recombinant VSV, most of them immediately reverted to the wild-type (WT) sequence after a single passage. However, a single passage of recombinant virus D268L resulted in a pseudorevertant with a second mutation, L271P. Globally, this work demonstrates that these acidic residues ensure a correct activation of G at low pH and that the stability of helix F has to be tightly regulated since both its destabilization and overstabilization are detrimental to the virus.

MATERIALS AND METHODS

Cells and antibodies. BSR, clones of BHK-21 (baby hamster kidney; ATCC CCL-10), and HEK-293T (human embryonic kidney expressing simian virus 40 T antigen [SV40T]; ATCC CRL-3216) cells were grown in Dulbecco's modified Eagle's medium (DMEM) supplemented with 8% fetal calf serum (FCS).

Mouse monoclonal antibody directed against G ectodomain was supplied by KeraFAST (8G5F11); mouse monoclonal antibody directed against the C-terminal intraviral part of G was supplied by Sigma (P5D4). Rabbit polyclonal antibodies raised against purified glycoprotein G were produced at the Institut de Neurobiologie Alfred Fessard (INAF) platform (CNRS, Gif-sur-Yvette, France).

Plasmids and cloning. Mutants were constructed, starting from the cloned VSV G gene (Indiana Mudd-Summer strain) in plasmid pcDNA3.1, by PCR overlap extension mutagenesis. Briefly, forward and reverse primers containing the desired mutation were combined separately with one of the primers flanking the G gene to generate two different intermediate PCR products. These two G gene fragments overlap in the region containing the mutation and were used as a template in a third PCR to generate the full-length G gene containing the mutation. The sequences of the primers which hybridize to the ends of G gene are the following: 5′ VSV G, 5′-CTAGAGCGGCCGCATGAAGTGCCTTTTGTAC-3′; 3′ VSV G, 5′-TGCAGGATATCTTACTTTCCAAGTCGGTTC-3′.

The sequences of mutant-G primers are the following (only the sense strand is reported): for D268L, 5′-CCATCTCAGACCTCAGTGCTTGTA AGTCTAATTCAGG-3′; D268N, 5′-CCATCTCAGACCTCAGTGAATG TAAGTCTAATTCAGG-3′; D274N, 5′-GATGTAAGTCTAATTCAGAA CGTTGAGAGGATCTTGG-3′; E276Q, 5′-GTCTAATTCAGGACGTTC AGAGGATCTTGGATTATTC-3′; D393N, 5′-GATTGGACATGGTATG TTGAACTCCGATCTTCATCTTAG-3′; D395N, 5′-CATGGTATGTTG AACTCCGTTCTTCATCTTAGCTCAAAG-3′.

Starting from the constructed simple mutants, an additional two-step PCR-based site-directed mutagenesis was performed in order to obtain the double mutants D274N/D395N and E276Q/D393N. The different constructions were then subcloned from pcDNA3.1 to pCAGGS by PCR amplification.

Transfections. For fusion assays and indirect immunofluorescence, BSR cells, grown in six-well plate at 70% confluence, were transfected by the phosphate calcium method (5 μg of the appropriate plasmid per well).

For endo-β-*N*-acetylglucosaminidase H (endo H) resistance, BSR cells grown in six-well plates at 70% confluence were first infected by vaccinia virus expressing T7 polymerase (vTF7-3) at a multiplicity of infection (MOI) of 5. Following 1 h of incubation, cells were washed with DMEM and transfected by the phosphate calcium method (5 μg of the appropriate plasmid per well).

For G sedimentation analysis and cytometry experiments, HEK-293 cells grown in six-well plates at 70 to 80% confluence were transfected with 2 μg of the appropriate plasmid using Lipofectamine 2000 (Invitrogen) according to the manufacturer's instructions.

For pseudotyped virus production, HEK-293 cells were grown in 10-cm dishes; they were transfected by 6 μg of the appropriate plasmid with polyethylenimine (PEI; Sigma-Aldrich).

Indirect immunofluorescence. BSR cells plated on glass coverslips at 70% confluence were transfected with pcDNA3.1 plasmids encoding WT or mutant G, as described above. At 24 h after transfection, cells were fixed with 4% paraformaldehyde in 1× phosphate-buffered saline (PBS) for 15 min and then permeabilized or not in 0.1% Triton X-100 in PBS for 5 min. Glycoprotein was detected by using a mouse monoclonal anti-G ectodomain antibody (8G5F11; KeraFAST). Goat anti-mouse Alexa Fluor 488 (Invitrogen) was used as a secondary antibody. Images were acquired with a Zeiss Axiovert 200 fluorescence microscope (Carl Zeiss MicroImaging, Inc., Germany) equipped with a 63× lens (oil) connected to a charge-coupled-device camera and a computer equipped with AxioVision software. Excitation was performed at 488 nm (Alexa Fluor 488). Cell nuclei were stained with 4′,6′-diamidino-2-phenylindole (DAPI).

Cell surface expression. In order to quantify the expression of G protein on the cell surface, HEK-293 cells plated on six-well dishes at 70% confluence were transfected as described above. At 24 h after transfection, cells were collected by scraping into 1 mM EDTA-PBS, followed by centrifugation at 600 × *g* for 5 min. Cells were incubated with a 1:2,000 dilution of mouse monoclonal anti-G ectodomain antibody (8G5F11; KeraFAST) in PBS on ice for 1 h. Cells were washed twice in PBS, fixed at 4°C in paraformaldehyde, incubated with a 1:100 dilution of goat anti-mouse Alexa Fluor 488 (Invitrogen) on ice for 1 h, and rinsed in PBS. After resuspension in 500 ml of 0.5 mM EDTA-PBS, the fluorescence of 10,000 cells from each population was determined by flow cytometry using a BD Accuri C6 fluorescence-activated cell sorter (FACS). The mean fluorescence intensity (MFI) of the transfected cells expressing G was quantified by flow cytometry. The relative cell surface expression of transfected cells was determined as follows: (MFI for the mutant)/(MFI for the WT). For each mutant, the percentage given in Fig. 2C is the average of three independent experiments.

Endo H sensitivity. At 20 h after transfection, BSR cells were starved of methionine and cysteine for 90 min. Cells were then pulse-labeled with 50μ Ci of [^{35}S]Met-Cys for 5 min. The medium was then replaced by prewarmed DMEM supplemented with a 20-fold excess of nonradioactive Met-Cys for a variable chase period (10 to 105 min). Cells were lysed with TD buffer (137 mM NaCl, 5 mM KCl, 0.7 mM Na_2HPO_4, and 25 mM Tris-HCl [pH 7.5]) plus 1% CHAPS (3-[(3-cholamidopropyl)-dimethylammonio]-1-propanesulfonate), and G protein was selectively immunoprecipitated by a rabbit polyclonal anti-G antibody. The samples were denatured by the denaturation buffer supplied by the manufacturer (New England BioLabs). Half of the samples were treated by 0.5 U of endo-β-*N*-acetylglucosaminidase H (endo H) in the reaction buffer supplied by

the manufacturer for 1 h at 37°C. Equal quantities of the treated and untreated samples were denatured in Laemmli buffer and analyzed by SDS-PAGE, followed by autoradiography.

Cell-cell fusion assay. BSR cells plated on glass coverslips at 70% confluence were cotransfected with pCAGGS plasmids encoding the WT G or mutant G and a plasmid encoding the phosphoprotein of rabies virus fused to green fluorescent protein (P-GFP) (25). At 24 h after transfection, cells were incubated with fusion buffer (DMEM–10 mM morpholineethanesulfonic acid [MES]) at various pHs (from 5.0 to 7.0) for 10 min at 37°. Cells were then washed once and incubated with DMEM–10 mM HEPES–NaOH buffered at pH 7.4 and 1% bovine serum albumin (BSA) at 37°C for 1 h. Cells were fixed with 4% paraformaldehyde in 1× PBS for 15 min. Cell nuclei were stained with DAPI, and syncytium formation was analyzed with a Zeiss Axiovert 200 fluorescence microscope equipped with a 20× lens.

In some experiments, fusion activity was assayed after incubation of the cells in DMEM–10 mM Tris-HCl buffered at pH 8.5 at 20°C for 10 min before the pH was lowered with DMEM–25 mM MES–NaOH adjusted at the required pH.

Oligomerization assay. The oligomeric state of the G protein was determined by sucrose gradient centrifugation. HEK-293 cells were transfected by the Lipofectamine method as described above. At 24 h after transfection, cells were collected by scraping into PBS, followed by centrifugation at 2,500 rpm for 5 min. Cell lysates were prepared using 100 mM NaCl containing either 50 mM MES-NaOH (for pH 5 to 6.5) or 50 mM Tris-HCl (for pH 7 and 7.5) plus 0.5% NP-40 at 4°C for 30 min; they were clarified by centrifugation at 10,000 rpm for 2 min and overlaid on a 5 to 20% continuous sucrose gradient in 100 mM NaCl and 50 mM Tris-HCl [pH 7.0 or 7.5] or 100 mM NaCl and 50 mM MES-NaOH [pH 5.0, 5.5, 6.0, or 6.5], plus 0.1% Triton supplemented with an antiprotease cocktail. Following centrifugation at 35,000 rpm for 16 h in an SW41 rotor (Beckman Coulter, Brea, CA), 12 equal fractions were collected manually from the bottom of the gradient. When required, the pH of each fraction was adjusted to a pH of ~7.5, and G protein was immunoprecipitated using a rabbit polyclonal anti-G antibody at 4°C for 2 h; immune complexes were immobilized on protein A-Sepharose beads for 1 h at 4°C, washed three times, denatured, and analyzed by SDS-PAGE. Immunoprecipitated G was revealed by Western immunoblotting with a mouse monoclonal antibody (P5D4).

Pseudotype complementation assay. VSVΔG-GFP is a recombinant VSV which was derived from a full-length cDNA clone of the VSV genome (Indiana serotype) in which the coding region of the G protein was replaced by a modified version of the GFP gene and pseudotyped with the VSV G protein (26, 27). VSVΔG-GFP was propagated on HEK-293T cells that had been transfected with pCAGGS-VSV-G.

For this assay, HEK-293T cells at 70 to 80% confluence were transfected by pCAGGS encoding WT VSV G, using the PEI method as described above. At 24 h after transfection, cells were infected with VSVΔG-GFP at an MOI of 0.1. Supernatant was collected after 24 to 36 h of infection when typical VSV cytopathic effects were observed. Stocks of recombinant viruses pseudotyped by VSV G protein were stored at −80°C. The infectious titers of the recovered viruses were determined on nontransfected cells by counting cells positive for GFP expression.

For the complementation assay by mutant glycoproteins, the protocol was similar to that described above except that cells were transfected with a pCAGGS plasmid encoding mutant G. In this case, 2 h after infection by the virus pseudotyped by WT G (MOI of 3), cells were washed three times with DMEM to remove residual viruses from the inoculum and incubated with DMEM–1% fetal bovine serum (FBS) for the rest of the infection period.

Recovery of recombinant virus. Plasmid pVSV-FL(+) expressing the 11,161-nucleotide (nt) positive-strand full-length VSV RNA sequence and plasmids pBS-N, pBS-P, and pBS-L, respectively, encoding N, P, and L proteins were kindly provided by John K. Rose (Yale University, New Haven, CT, USA). The mutant G genes of the VSV Indiana serotype (Mudd-Summers strain) were inserted into the original full-length genomic plasmid pVSV-FL(+) (28) using two unique sites of pVSVFL(+), MluI in the 5′ noncoding sequence of the glycoprotein (G) gene and NheI present in a sequence introduced between G and L, after removal of the corresponding VSV Indiana Mudd-Summers G gene. Recombinant VSV was recovered as described by Schnell et al. (29). The plasmids were transfected into the cells with Lipofectamine 2000 (Invitrogen) in the presence of 10 μg/ml 1-β-D-arabinofuranosylcytosine (araC; Sigma).

Two mutants (D393N and D274N) could not be generated spontaneously. The recovery of these mutants was supported by expression of functional WT VSV G protein in *trans* from a plasmid (pcDNA3.1 Gwt) which was cotransfected with plasmids pVSV-FL(+), pBS-N, pBS-P, and pBS-L.

Electron microscopy. Purified virions were diluted in 150 mM NaCl in either 50 mM Tris-HCl, pH 8.0, or 50 mM 3-(*N*-morpholino)propanesulfonic acid (MOPS) at pH 5.5. Samples were then adsorbed onto airglow discharge carbon-coated grids and stained with sodium phosphotungstic acid adjusted to the sample pH (8.0 or 5.5). Images were recorded in an electron microscope (model CM12; Philips) operated at 80 kV, with a nominal magnification of 35,000.

RESULTS

Mutations of acidic residues putatively playing the role of pH-sensitive switches have no major effect on glycoprotein transport. In the prefusion state of VSV G, there are some solvent-exposed acidic residues (Fig. 1A, B, and C) which, as a result of the low-pH-induced structural transition, are brought close together in the postfusion state (Fig. 1D). In the postfusion trimer, these residues are protonated and form intra- and interprotomer hydrogen bonds (Fig. 1D). Their deprotonation, upon pH increase, is supposed to induce strong repulsive forces that destabilize the postfusion trimer and initiate the conformational change back toward the prefusion state. Among these residues, the three Asp 268 residues point toward the axis of the trimer and are buried in the hydrophobic environment of the postfusion trimeric interface (Fig. 1D). Another destabilization of the trimer is also expected by the simultaneous deprotonation of Asp 274 from one protomer and Asp 395 from the neighboring protomer, which are facing each other (Fig. 1D). Finally, the deprotonation of both Glu 276 and Asp 393, which are also facing each other, might create a repulsive force between helices H and F of the same protomer (Fig. 1D).

We decided to replace these acidic residues either by the corresponding amide residue (i.e., Asp by Asn and Glu by Gln) or, in the case of Asp 268, by hydrophobic Leu that was supposed to stabilize the contact between central helices F in the trimer. As a consequence, we constructed six single mutants (D268N, D268L, D274N, D395N, E276Q, and D393N) and two double mutants (D274N/D395N and E276Q/D393N). It is worth noting that replacement of Asp 268 by Asn creates a sequon (Asn-Val-Ser) that constitutes a new potential glycosylation site.

BSR and HEK cells were transfected with pcDNA3.1 plasmids, allowing the expression of wild-type (WT) and mutant glycoproteins. Protein expression and cell surface localization of mutant G proteins were analyzed by indirect immunofluorescence microscopy on both permeabilized and nonpermeabilized BSR cells (Fig. 2A and B). The amount of G protein present on the surface of HEK cells was quantified using flow cytometry (Fig. 2C). Mutant glycoproteins were all surface expressed at levels varying from 54 to 113% of WT VSV G (Fig. 2B and C). This indicated that these mutant glycoproteins, being able to leave the endoplasmic reticulum (ER), have the characteristics of folded proteins (30). The

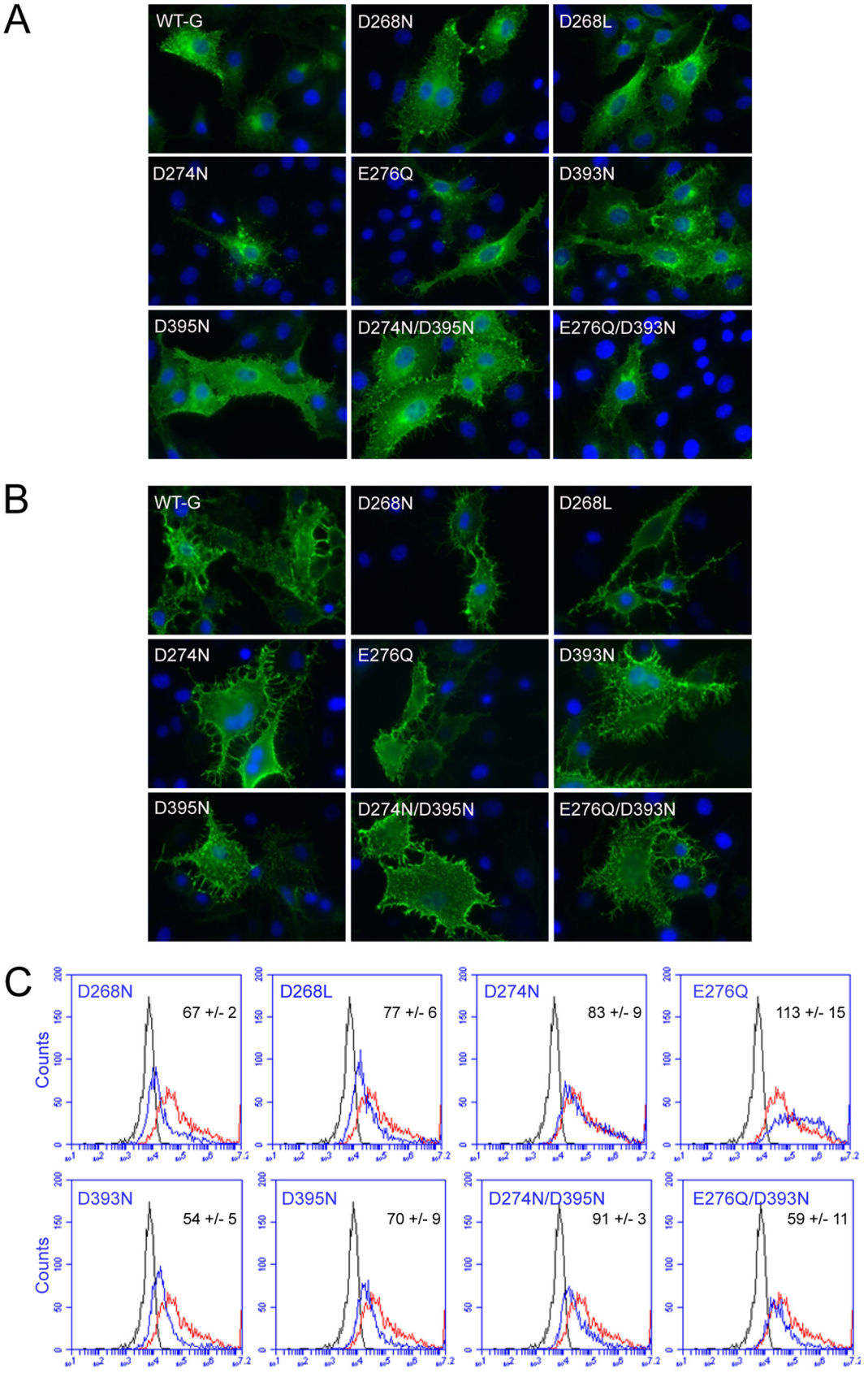
A
WT-G
D268N
D268L
D274N
E276Q
D393N
D395N
D274N/D395N
E276Q/D393N
B
WT-G
D268N
D268L
D274N
E276Q
D393N
D395N
D274N/D395N
E276Q/D393N
C
D268N
67 +/- 2
D268L
77 +/- 6
D274N
83 +/- 9
E276Q
113 +/- 15
D393N
54 +/- 5
D395N
70 +/- 9
D274N/D395N
91 +/- 3
E276Q/D393N
59 +/- 11
Counts
Counts

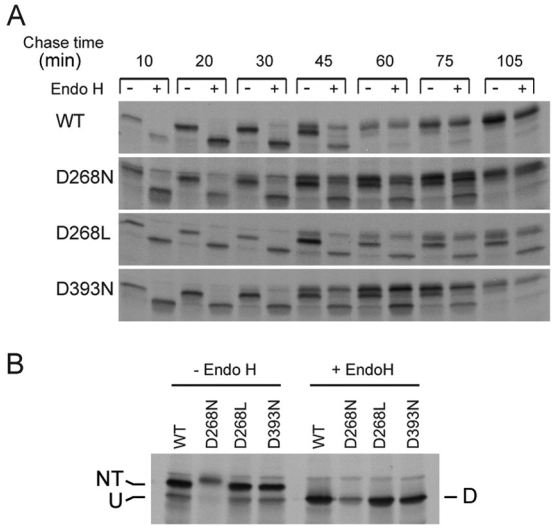

FIG 3 (A) Kinetics of endo H acquisition for WT VSV G and mutants D268N, D268L, and D393N. Transfected BSR cells were pulse-labeled for 5 min by [^{35}S]Met-Cys and then chased for up to 105 min. G was then immunoprecipitated and incubated in the presence or absence of endo H. The samples were then analyzed by SDS-PAGE under reduced conditions. (B) Mutant D268N has an extra oligosaccharide side chain; untreated mutant D268N has a slower migration on SDS-PAGE while migration of the endo H-treated mutant is similar to that of the WT. The experiment was performed as in described in panel A with a chase of 20 min. D, endo H deglycosylated G; U, unglycosylated G; NT, nontrimmed G. All gels are representative examples from three independent experiments.

modest but significant reduction in surface expression of some mutants might reflect slightly lower expression levels, slower transport, or partial retention of the glycoprotein in the ER due to less efficient folding.

To get better insight on this question, we also analyzed the kinetics of acquisition of endoglycosidase H (endo H) resistance for WT G and some of the mutants. Acquisition of endo H resistance by the sugar chains indicates the arrival of glycoproteins in the medial cisternae of the Golgi apparatus (31). Transfected cells were pulse-labeled for 5 min by [^{35}S]Met-Cys and then chased for up to 105 min (Fig. 3A). G was then immunoprecipitated from the cell extract and incubated in the presence or absence of endo H. The samples were then analyzed by SDS-PAGE under reduced conditions (Fig. 3A). WT G was fully endo H resistant after about 60 min. Mutant D393N (which exhibited the lowest surface expression) and mutant D268N had very similar kinetics of endo H resistance acquisition and were both fully endo H resistant after about 105 min. On the other hand, mutant D268L was more slowly transported (as only ~50% of G was endo H resistant 105 min after synthesis). The endo H experiments also revealed that the sequon created by the mutation D268N was indeed recognized by the cellular glycosylation machinery and that mutant D268N had an extra oligosaccharide chain (Fig. 3B).

Fusion properties of the glycoprotein mutants. Fusion properties of mutant glycoproteins were analyzed in a cell-cell fusion assay. For this, BSR cells were cotransfected with a plasmid encoding the RABV phosphoprotein fused with the green fluorescent protein (P-GFP) and the plasmid encoding WT or mutant glycoproteins (32). P-GFP is unable to diffuse passively in the nucleus (25), which, on the one hand, allows an easy detection of the transfected cells and, on the other, the counting of the number of syncytia they formed upon fusion (Fig. 4). At 24 h after transfection, the cells were exposed for 10 min (at 37°C) to DMEM adjusted to the required pH, which was then replaced by DMEM buffered at pH 7.4. The cells were then kept at 37°C for 1 h before fixation.

Cells expressing wild-type G protein formed massive syncytia when exposed to low pH, between 5.5 and 6.3 (Fig. 4). Small syncytia (containing less than 10 nuclei) were still observed at pH 6.5 (Fig. 4) and even at higher pH (data not shown). In striking contrast, replacement of Asp 268 by Leu or Asn led to complete inhibition of cell-cell fusion, even at pH 5 (Fig. 4). Cells expressing G mutants having mutations in positions 274, 276, 393, and 395 were all able to form syncytia when exposed at low pH, however with various efficiencies (Fig. 4). Mutant E276Q had a fusion phenotype identical to that of WT G. Mutant D395N had the same pH dependence as WT G; however, massive syncytia were observed only at pH 5.5 or below. For mutants D274N, D393N, and the two double mutants, fusion was less efficient: syncytia remained small and were detected strictly below pH 6.0 (Fig. 4).

Oligomerization status of mutant glycoproteins. In the case of WT G, the prefusion trimer, although detected at the viral surface (16), is not stable in solution and only monomers are detected at high pH (14, 17). On the other hand, at low pH, the postfusion trimer is stable. Monomers and postfusion trimers can be easily separated in a sucrose gradient (14) (Fig. 5): monomeric G is recovered in the upper fractions (10 and 11), while trimeric G is found in fractions 8 and 9. The transition pH is defined as the value at which monomeric and trimeric G are found in equal amounts.

We analyzed the oligomeric status of WT G and the mutants using this property in a sucrose gradient after detergent solubilization (Fig. 5). For WT G, monomers were detected above pH 7, and trimers were observed below pH 6. At pH 6.5, both trimers and monomers were observed. Similar results were ob-

FIG 2 Effect of the mutations on VSV G expression and transport in BSR and HEK cells. (A) Expression and subcellular localization of G proteins in BSR cells. Epifluorescence images of transfected cells are shown. At 24 h posttransfection, cells were permeabilized and fixed, and G was detected by immunostaining with a monoclonal antibody to VSV G (8G5F11; KeraFAST), which was subsequently detected by using a goat anti-mouse IgG secondary antibody conjugated to Alexa Fluor 488. Nuclei were stained with DAPI. (B) Surface expression of G proteins in BSR cells. Epifluorescence images of nonpermeabilized transfected cells are shown. At 24 h posttransfection, cells were fixed, and G was detected by immunostaining with a monoclonal antibody to VSV G (8G5F11; KeraFAST) and a goat anti-mouse IgG secondary antibody conjugated to Alexa Fluor 488. (C) Surface expression of G in HEK cells. HEK cells were collected into PBS containing 1 mM EDTA at 24 h posttransfection and pelleted by centrifugation (600 × *g* for 5 min). The surface G protein expression was detected with a monoclonal antibody to VSV G (8G5F11; KeraFAST) and a goat anti-mouse IgG secondary antibody conjugated to Alexa Fluor 488. A total of 10,000 cells were counted by flow cytometry. In each frame, the black curve corresponds to the fluorescence of untransfected cells, the red curve corresponds to the fluorescence of cells transfected by pCAGGS plasmids encoding WT G, and the blue curve corresponds to the fluorescence of cells transfected by pCAGGS plasmids encoding the indicated mutant. In each frame, the surface expression of mutant G is expressed as a percentage of that of WT G. Values are the average of three independent experiments ± the standard deviations.

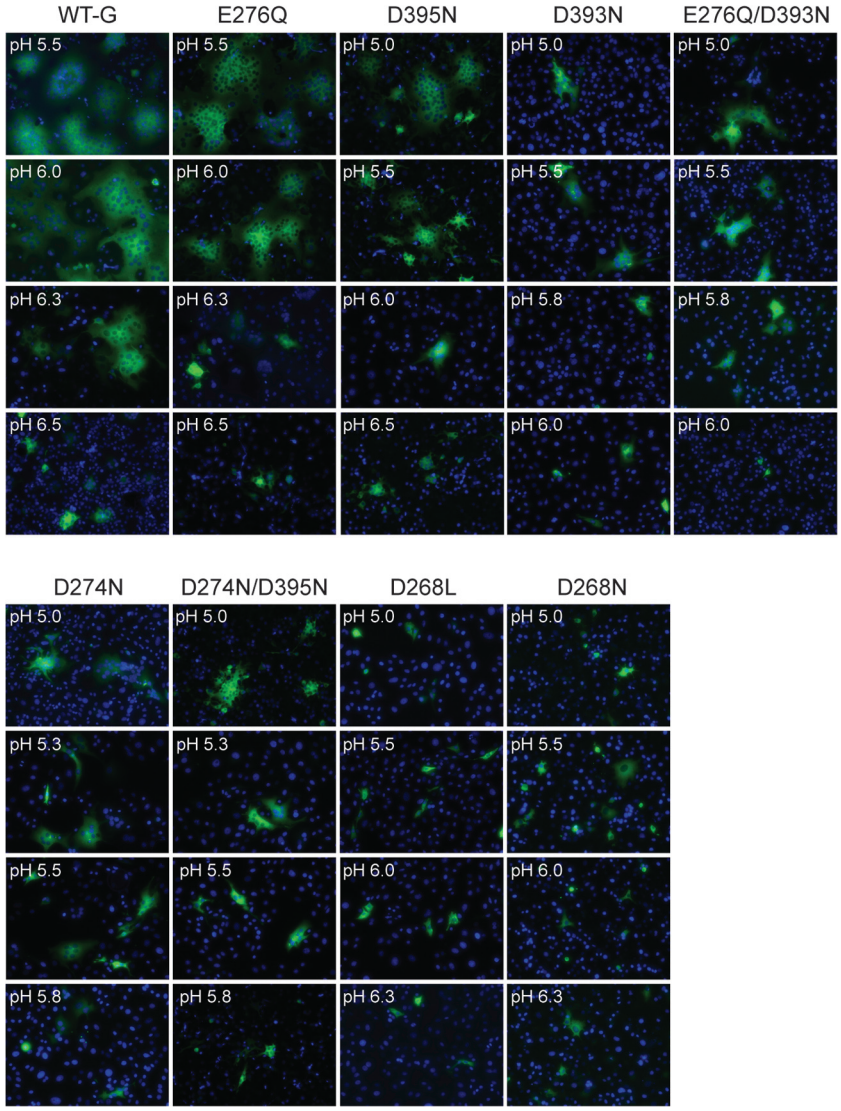

FIG 4 Fusion activity of WT and VSV G mutants analyzed in a cell-cell fusion assay. BSR cells were transfected with plasmids expressing VSV G (either WT or mutant) and P-GFP, allowing an easy observation of syncytia. At 24 h posttransfection, the cells were exposed for 10 min to DMEM adjusted to the indicated pH, which was then replaced by DMEM at pH 7.4. The cells were then kept at 37°C for 1 h before fixation. For each glycoprotein (either WT or mutant), only the representative pHs are shown, according to the associated fusion phenotype. The mutants are presented in the figure in order of decreasing fusion efficiency, starting with WT G. Nuclei were stained with DAPI. All images are representative examples from at least three independent experiments.

served with G mutants E276Q, D395N, D274N/D395N, and E276Q/D393N. A slight destabilization of the postfusion trimer was observed for mutants D393N and D274N as the postfusion trimer was observed strictly below pH 6.5. In striking contrast, the postfusion trimer was still detected at pH 7 for mutant D268L, whereas only monomers were detected with mutant D268N, which was not a surprise as the addition of an oligosaccharide chain on the asparagine clearly interferes with the formation of the postfusion trimer.

High-pH treatment allows partial recovery of the fusion activity of mutant D268L. The latter experiment indicated that the postfusion state of mutant D268L was more stable than that of WT G at high pH. We hypothesized that the inability of these mutants to induce syncytium formation under standard experimental conditions (i.e., by lowering the pH from ~7.2 to 6) might be due to the fact that most of the glycoproteins were still in a postfusion form at pH 7.2. Therefore, we decided to incubate cells expressing mutant glycoproteins at pH 8.5 and 20°C for 10 min before lowering the pH below 6. After this treatment, small syncytia were clearly detected for cells expressing mutant D268L (Fig. 6), which was not the case for cells expressing mutant D268N (Fig. 6). This definitively confirmed that mutation D268L stabilized the trimeric postfusion conformation.

Characterization of the mutant glycoproteins' ability to sustain infection using a VSV pseudotype. To examine whether the mutant glycoproteins were able to sustain viral infection, we used a recombinant VSV (VSVΔG-GFP) in which the G envelope gene was replaced by the green fluorescent protein (GFP) gene and which was pseudotyped with the VSV G glycoprotein (26, 27). This pseudotyped recombinant was used to infect HEK cells (at an

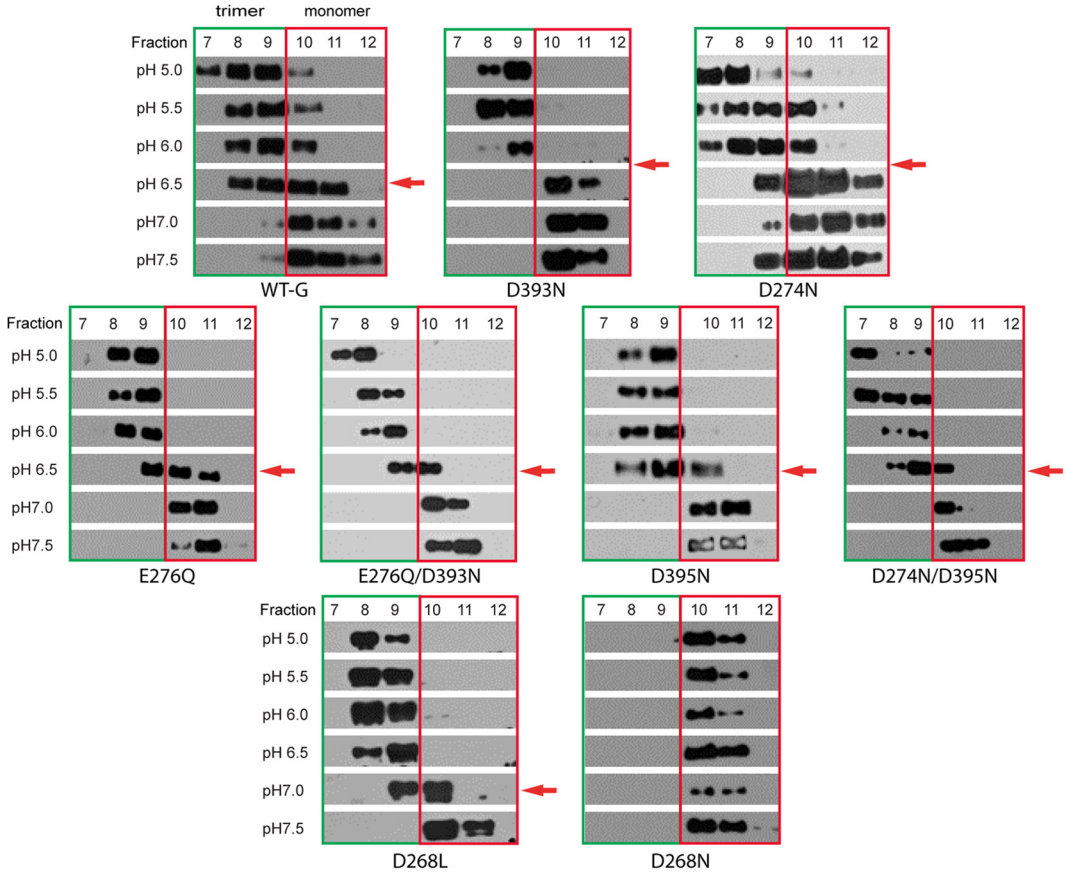

FIG 5 Oligomerization assay of WT and mutant G. At 24 h after transfection, HEK cells were lysed, and the cellular extracts were overlaid on a 5 to 20% continuous sucrose gradient in 100 mM NaCl–0.1% Triton, adjusted to the required pH. After centrifugation for 16 h at 35,000 rpm, 12 fractions were collected from the bottom of the gradient. For each fraction, G protein was immunoprecipitated using rabbit polyclonal anti-G antibody. Immunoprecipitated proteins were analyzed by Western immunoblotting with a mouse monoclonal antibody directed against the C-terminal, intraviral, part of G (P5D4; Sigma). G found in fractions 10 and 11 (red box) corresponds to a monomer, whereas G found in fractions 7 to 9 (green box) corresponds to the trimer. For each mutant (except D268N, which is always recovered as a monomer), the red arrow indicates the pH of the transition, which is pH 6.5 for WT G and mutants E276Q, D395N, D274N/D395N, and E276Q/D393N, between pH 6 and pH 6.5 for mutants D393N and D274N, and pH 7 for mutant D268L. All the data presented in this figure are representative examples from at least three independent experiments.

MOI of 3) either transfected or not transfected by a plasmid encoding WT or mutant glycoproteins.

After 16 h, the infected cell supernatant was collected, and the infectivity of the pseudotyped particles present in the supernatant was analyzed in HEK cells (Fig. 7). The infectivity was determined by counting the cells expressing GFP by flow cytometry at 16 h postinfection. It appeared that mutant E276Q could rescue the infectivity of VSVΔG-GFP at a level similar to that of WT G. The other mutants were all affected although to different levels. Mutants D395N and D274N were the least affected (exhibiting, respectively, ~10- and ~20-fold less infectivity than viruses pseudotyped by WT G). Mutants D268L and D274N/D395N were slightly more affected (exhibiting, respectively, ~50- and ~70-fold less infectivity than viruses pseudotyped by WT G). Mutation D393N appeared to be extremely detrimental as both mutant D393N and E276Q/D393N only poorly rescued the infectivity of VSVΔG-GFP, and were, respectively, ~400- and 180-fold less efficient than WT G. Finally, mutant D268N exhibited more than 4,000-fold lower infectivity than viruses pseudotyped by WT G, and, in fact, its infectivity could not be distinguished from that of nonpseudotyped particles.

Attempt to generate recombinant viruses. As several mutants rescued the infectivity of VSVΔG-GFP, we tried to generate recombinant VSV containing mutations D268L, D274N, E276Q, D393N, and D395N. We easily generated recombinant VSV expressing the E276Q mutation (VSV G.E276Q). We also generated recombinant VSV G.D395N which, after sequence analysis revealed a reversion to an aspartic residue in position 395. The reversion was evidenced by the fact that the codon encoding the aspartic acid was distinct from the one found in the wild-type sequence of the G gene (Table 1).

As the other mutants (VSV G.D268L, VSV G.D274N, and VSV G.D393N) were not generated spontaneously, we employed a complementation strategy to support their growth (23, 33). Briefly, the recovery of the recombinant VSV was supported by expression of functional WT VSV G protein in *trans* from a transfected plasmid. To generate virus particles containing only the fusion-defective VSV G expressed from the viral genome, viruses present in the supernatant were amplified in cells that lack the *trans*-complementing VSV G plasmid.

Using this approach, we recovered infectious viruses for each mutant. However, for mutants D274N and D393N, once again,

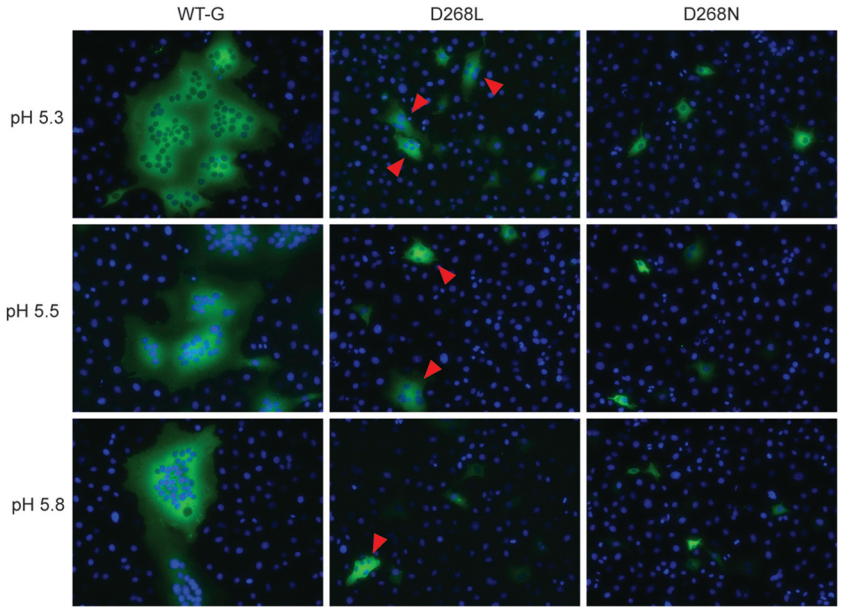

FIG 6 Preincubation of cells expressing mutant D268L at pH 8.5 allows a partial recovery of the fusion activity. BSR cells were transfected by a plasmid expressing either WT G, mutant D268L, or mutant D268N. At 24 h posttransfection, the cells were exposed for 10 min to DMEM adjusted to pH 8.5 at 20°C. The cells were then exposed for 10 min to DMEM adjusted to the indicated pH. The cells were then kept at 37°C in DMEM, pH 7.4, for 1 h before fixation. Small syncytia, indicated by red triangles, were clearly observed with mutant D268L, which was not the case with mutant D268N. Nuclei were stained with DAPI.

sequence analysis revealed a reversion toward the wild-type sequence (i.e., D in position 274 and D in position 393, respectively). In both cases, the reversions were evidenced by the fact that the codon encoding the aspartic acid was distinct from the one found in the wild-type sequence of the G gene (Table 1). In the case of mutant D268L, sequence analysis revealed a single additional coding change in the genome, resulting in the replacement of leucine 271 with a proline, leading to the double mutant VSV G.D268L/L271P.

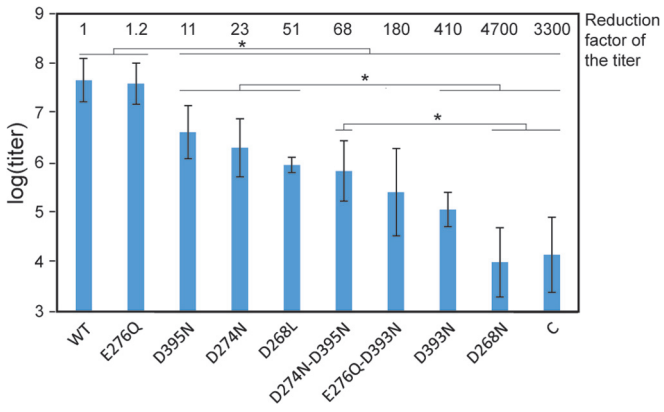

FIG 7 Infectivity of VSVΔG-GFP pseudotyped by mutant glycoproteins. VSVΔG-GFP pseudotyped with the WT VSV G glycoprotein was used to infect cells transfected with the indicated mutant at an MOI of 3. After 16 h, VSVΔG-GFP pseudotyped by mutant glycoproteins present in the supernatant was used to infect HEK cells. After 16 h of infection, HEK cells which were expressing GFP were counted by flow cytometry. The MOI was then determined using the following formula: MOI = $-\ln(p(0))$, where $p(0)$ is the proportion of noninfected cells (40, 41). The titer of the inoculum was then calculated from the MOI. For each mutant, the bar graph gives the mean of the log(titer) ± standard deviation calculated from three independent experiments. C represents the nonpseudotyped control. Above each bar, the reduction factor of the titer (compared top VSVΔG-GFP, pseudotyped by WT G) is indicated. The asterisk denotes a statistically significant difference between two groups of pseudotyped viruses ($P = 0.05$, rank test).

Characterization of VSV G.D268L/L271P. We compared one-step growth curves of the WT and mutants VSV G.E276Q and VSV G.D268L/L271P in BSR cells infected at an MOI of 3. The growth curve of mutant E276Q was similar to that of the WT virus. For mutant VSV G.D268L/L271P, the titer was reduced by about one order of magnitude after 6 h of infection (Fig. 8A). The virus released in the culture medium after 18 h was also purified and analyzed by SDS-PAGE (Fig. 8D). Similar amounts of viral particles were found in the supernatant of cells infected by either WT VSV or VSV G.D268L/L271P, suggesting that the particles of the mutant were less infectious than those of the WT. However, the average number of glycoproteins per virion was also apparently the same for both viruses.

We decided to further characterize the properties of mutant glycoprotein D268L-L271P and of the mutant harboring the single mutation L271P. BSR cells were therefore transfected by plasmids allowing the expression of both mutant glycoproteins. The fusion properties of both mutants were assayed. Mutant D268L/L271P has fusion properties that are similar to those of the WT, whereas mutant L271P has fusion properties that were much

TABLE 1 Codons of WT, mutant, and revertant virus

Mutant	Original codon[a]	Mutated codon[b]	Revertant codon[c]
D274N	GAC	AAT	GAT
D393N	GAC	AAT	GAT
D395N	GAT	AAC	GAC

[a] Wild-type sequence, encoding D.
[b] Mutant sequence, encoding N.
[c] Revertant sequence, encoding D, found in the recovered virus.

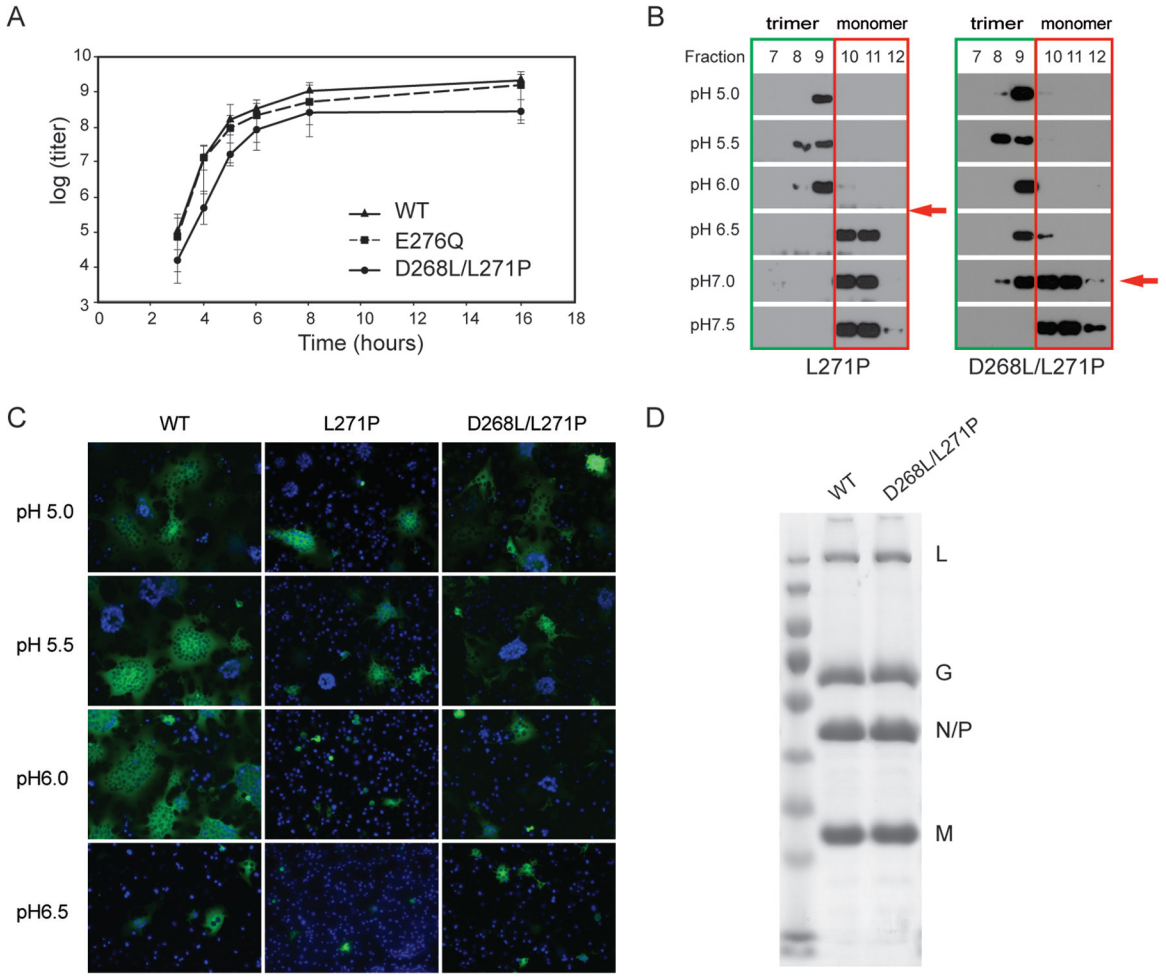

FIG 8 Characterization of the properties of recombinant viruses VSV G.E276Q and VSV G.D268L/L271P. (A) One-step growth curves of WT VSV, VSV G.E276Q, and VSV G.D268L/L271P. BSR cells were infected at an MOI of 3, and samples were harvested for titration at the indicated times postinfection. Viral titers represent averages of titers from at least three independent experiments. (B) Oligomerization assay of mutants L271P and D268L/L271P. Experiments were performed as described in the legend of Fig. 5. The red arrow indicates the pH of the transition. (C) Fusion activity of mutants L271P and D268L/L271P analyzed in a cell-cell fusion assay. Experiments were performed as described in the legend of Fig. 4. (D) Protein profiles for WT VSV and VSV G.D268L/L271P. Virions were harvested from the supernatant of infected BSR cells at 18 h postinfection. Virion proteins were analyzed by SDS-PAGE and Coomassie blue staining. All the data presented in this figure are representative examples from at least three independent experiments.

more similar to those of mutants D393N, E276Q/D393N, and D274N/D395N (i.e., smaller syncytia and fusion detected only below pH 6.0) (Fig. 4 and 8C). We also analyzed the oligomeric status of both mutants as a function of pH. Mutant D268L/L271P has a behavior similar to that of D268L, with both trimers and monomers detected at pH 7, whereas the trimeric postfusion form of mutant L271P was detected at only pH 6 and below (Fig. 8B).

The ability of mutant L271P to pseudotype VSVΔG-GFP was also analyzed. This mutant was ~85-fold less efficient than WT in pseudotyping VSVΔG-GFP (data not shown).

Finally, the morphology of the spikes of VSV G.D268L/L271P at the surface of the virions was observed after negative staining (Fig. 9). At pH 8.0, both WT and mutant VSV G.D268L/L271P viral particles had the characteristic bullet shapes described in previous studies (16, 34–36) and exhibited the characteristic layers of spikes of ~8-nm width (Fig. 9A and B).

At low pH, viral particles were aggregated and fused, which made it very difficult to observe particle structure of isolated virions. The characteristic network of spikes in their low-pH postfusion conformation (16) was observed with WT G (Fig. 9C, E, and F). In the case of VSV G.D268L/L271P, close packing of spikes in their postfusion conformation was also observed, but no regular network could be detected (Fig. 9D, G, and H), which indicates that interactions between spikes are different for the mutant and for the WT virus.

DISCUSSION

Although several acidic residues have been speculated to play an important role as pH sensors in the reversibility of the VSV G structural transition (21, 37), experimental evidence for such a role was still lacking. In this study, we have mutated these acidic residues and have determined the consequences of the mutations for the glycoprotein conformational change, for the fusion properties, and for virus infectivity. The results are consistent with the fact that these residues are indeed keys in the regulation of the pH-dependent structural transition.

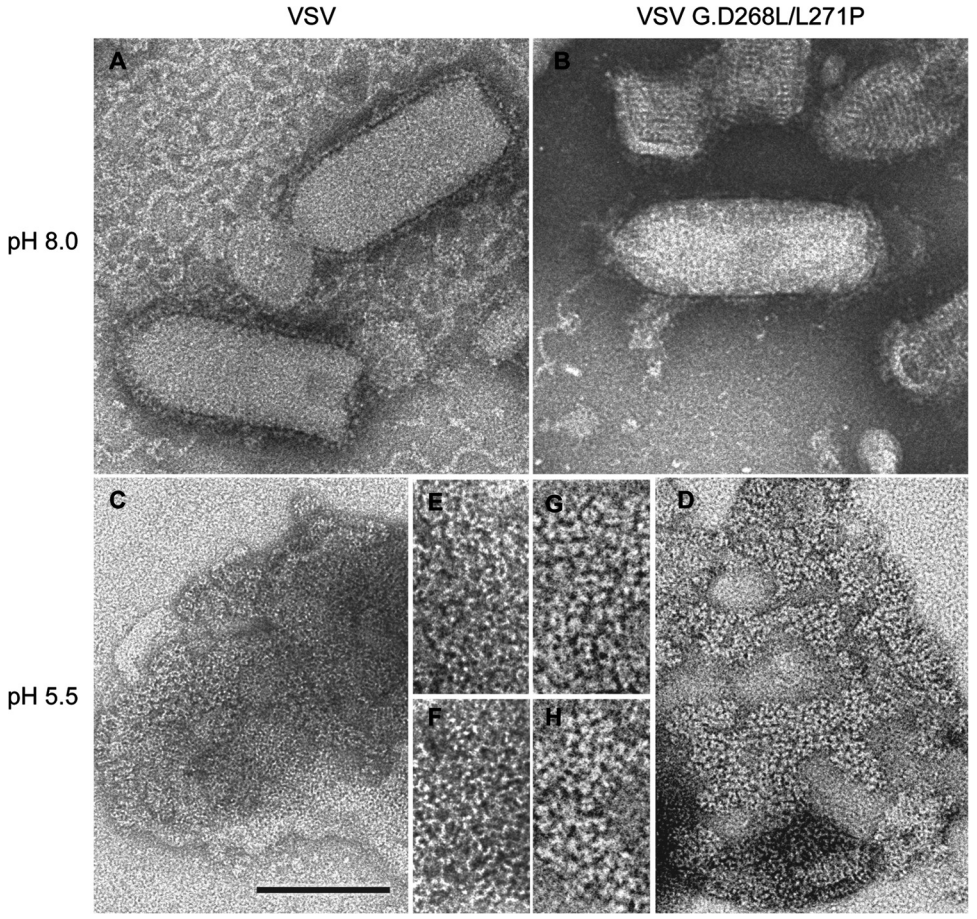

FIG 9 Morphology of negatively stained WT VSV (A, C, E, and F) and VSV G.D268L/L271P (B, D, G, and H) at pH 8.0 (A and B) and pH 5.5 (C to H). Panels E and F and panels G and H correspond to ×2 magnifications of the images in panels C and D, respectively. Images shown in panels A, B, C, and D are at the same scale. The scale bar in panel C represents 100 nm.

Asp 268 is a major pH-sensitive switch. Asp 268 is located in a segment that undergoes refolding during the low-pH-induced structural transition, leading to the extension of the central helix F (Fig. 10). As a consequence, in the postfusion trimer, the three Asp 268 residues are buried close to the 3-fold axis of the six-helix bundle (Fig. 1D), constituting the core of the trimer, which is essentially stabilized by hydrophobic interactions between helices. Clearly, the deprotonation of this residue at high pH induces repulsive forces that destabilize the postfusion trimer. As in the postfusion conformation, Asp 268 is buried in a hydrophobic environment; its pK_a is much higher than the pK_a of a solvent-exposed aspartic amino acid. As a consequence, the postfusion form still makes up the majority of the population up to pH 6.5 (16, 17).

Our work indeed demonstrates that Asp 268 is playing the role of a pH-sensitive molecular switch whose protonation/deprotonation regulates the structural transition of G. Depending on the amino acid which replaces Asp 268, two distinct phenotypes were observed.

First, the replacement of Asp 268 by an asparagine creates a sequon (Asn-Val-Ser), resulting in the addition of an extra oligosaccharide side chain, which, as a direct consequence, impedes the formation of a stable postfusion trimer. Consequently, mutant D268N is devoid of any fusion activity and is unable to pseudotype VSVΔG-GFP.

Second, the replacement of Asp 268 by a leucine increases the stability of the postfusion trimer at high pH. As a consequence, fusion is not observed under normal experimental procedures. However, the fusion activity can be partly restored upon preincubation of the cells at pH 8.5, which allows the mutant glycoprotein to recover its native prefusion state. This residual fusion activity explains why mutant D268L is still able to weakly pseudotype VSVΔG-GFP. Moreover, the fact that the transition back to the prefusion state is still observed (although at a higher pH) demonstrates that, besides Asp 268, other amino acids are involved in the pH-dependent relative stability of the pre- and postfusion states.

A finely tuned stability of the postfusion helix F. The mutation D268L is lethal for the virus. We used a previously described forward genetics approach (23, 33), and we isolated a compensatory mutation in position 271 (L271P) which is also located in the segment that refolds at low pH to elongate the central helix (Fig. 10). However, the compensation is only partial, and the infectivity per physical particle of VSV G.D268L/L271P is lower than that of the WT.

The D268L mutation alone overstabilizes helix F (by stabilizing the central trimer of helices), and the glycoprotein remains trapped in a postfusion state at high pH. As a consequence, fusion is severely impaired; the mutant glycoprotein is only weakly pseudotyping VSVΔG-GFP, and a recombinant virus harboring such a

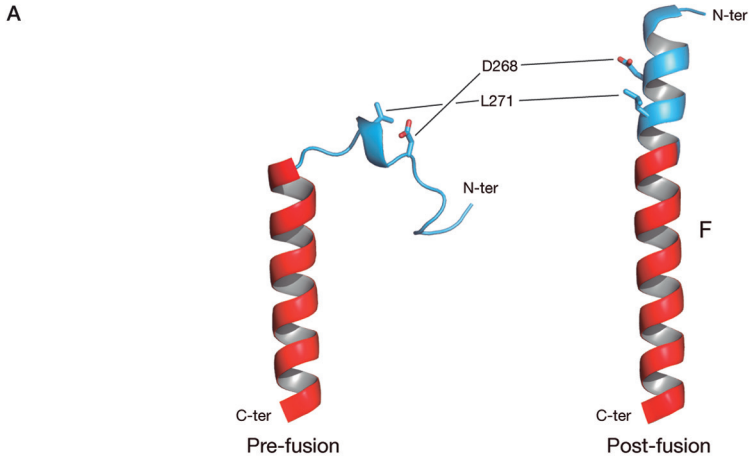

B

IND	264	QTSVDVSLIQDVERILDYSLCQETWSKIRA	293	384	LYMIGHGMLDSDLHLSS	400
MAR	264	QTSVDVSLIQDVERILDYSLCQETWSKIRA	293	384	LYMIGHGMLDSDLHKSS	400
ALA	264	QTSVDVSLILDVERMLDYSLCQETWSKVHS	293	384	LYMIGHGLLDSDLQKTS	400
COC	264	QTSVDVSLILDVERILDYSLCQETWSKIRS	293	384	LFMIGHGMLDSDLHKTS	400
NJ	268	EHATDISLISDVERILDYALCQNTWGKIEA	297	388	LHIIGTGEVDSDIKMER	404
CHAV	267	QSDGAQVLTSEIQRILDYSLCQNTWDKVER	296	388	WHLIGMGIVDNELHELS	404
ISF	267	LSEGVQTALWETDRLLDYSLCQNTWEKIDR	296	388	LYLLGMGIVDQDLQELS	404
PIR	266	ESEGARTLTWETQRMLDYSLCQNTWDKVSR	295	387	LYLIGAGIIDEDLHELD	403
PER	267	NSDGANTIAWETQRMLDYALCQSTWDKVQN	296	388	LYIIGTGLVDEDLQELS	404
MSV	267	QSEGSQTIAWETQRMLDYALCQNTWDKFER	296	388	LYAIGTGLIDQDIHELS	404
JUR	267	RSEGANTLTWETQRLLDYALCQNTWDKFDN	296	388	LYLVGMGMLDDEINALE	404
YBV	269	GSSPTRVVAWEMERIMDFALCQNVWDKVNR	298	390	FYLVGVGALDEDLIEMA	406
ABV	267	PDLRNIRMVWDLERVIENSLCQGTWDKIET	296	387	YYSVGIGKLDEDMITPD	403

FIG 10 (A) Ribbon representation of the segment corresponding to residues 264 to 293 of VSV G in its pre- and postfusion conformations. This segment is located in the trimerization domain and refolds during the structural transition. Its invariable part corresponding to residues 274 to 293, which is helical in both conformations, is shown in red. The part of the segment that refolds during the pH-dependent structural transition is depicted in cyan. Residues D268 and L271, both located in the refolding segment, are in stick representation. (B) Alignment of vesiculovirus glycoprotein sequences corresponding to VSV Indiana helices F (residues 264 to 293) and H (residues 384 to 400). Residues conserved among all vesiculoviruses are in red, acidic residues corresponding to VSV G residues 268, 274, 276, 393 and 395 are in cyan, and other acidic residues in helices F and H are in green. Virus names are abbreviated as follows: Ind, VSV Indiana (GenBank accession no. AAA48370.1); Mar, Maraba virus (GenBank accession no. AEI52254.1); Ala, vesicular stomatitis Alagoas virus (GenBank accession no. ACB47442.1); Coc, Cocal virus (GenBank accession no. ACB47437.1); NJ, VSV New Jersey (NCBI accession no. YP_009047084.1); ChaV, Chandipura virus (NCBI accession no. YP_007641380.1); Isf, Isfahan virus (NCBI accession no. YP_007641385.1); Pir, Piry virus (Swiss-Prot accession no. Q85213.1); Per, Perinet virus (GenBank accession no. AEG25354.1); Jur, Jurona virus (GenBank accession no. AEG25348.1); YBV, Yug Bogdanovac virus (GenBank accession no. AFH89679.1); MSV, Malpais Spring virus (GenBank accession no. AGI04017.1); ABV, American bat vesiculovirus TFFN-2013 (NCBI accession no. YP_008767242.1).

mutation is not viable. On the other hand, the single mutation L271P perturbs the final refolding of helix F due the helix-breaking property of the proline, and the trimeric postfusion state is detected only at pH 6 (i.e., ~0.5 pH unit lower than for WT G). As a consequence, fusion is also impaired and detected only below pH 6. Here, again, the mutant glycoprotein weakly pseudotyped VSVΔG-GFP. When both mutations are present, they compensate each other, resulting in a viable virus. Taken together, these data indicate that that the finely tuned stability of postfusion helix F is a key regulator for the functionality of the VSV fusion machinery. It both allows the fusion to occur at the correct pH and ensures the reversibility of the conformational change.

It is worth noting that although the fusion properties of the WT G and the D268L/L271P mutant are very similar, there are several phenotypic differences between them. First, the postfusion trimer of the mutant is still detected at pH 7, just as for single the mutant D268L. Furthermore, at low pH, mutant D268L/L271P in its postfusion conformation, although still making clusters, does not form the regular network observed with WT G. Residues D268 and 271, which are buried in the core of the postfusion state, cannot be involved in contact between spikes. This suggests that the presence of a proline in position 271 affects the trimeric interface of the postfusion state and consequently the relative orientation of the protomers at the top of the molecule, which in turn slightly modifies the interaction between spikes.

Several acidic residues regulate the structural transition and the fusion activity of VSV G. Mutations D393N and D274N also affect the fusion properties of G protein. For both of them, we observed a shift of the pH threshold of fusion from ~6.5 to ~6. Furthermore, even at lower pH, the resulting syncytia were always smaller than those observed with WT G. This weaker fusion activity is associated with a slight shift of the pK of the structural transition toward lower pH, which is observed for both mutants in a sucrose gradient. However, double mutants D274N/D395N and E276Q/D393N, which have fusion properties similar to those of mutants D274N and D393N, do not reveal a similar shift of the pKs of their structural transitions.

Our working hypothesis was that both pairs of acidic residues facing each other in the postfusion trimer (D274 and D395, on the one hand, E276 and D393, on the other) form two pH-sensitive

molecular switches. As a consequence, one would have expected similar phenotypes for mutants D274N and D395N, on the one hand, and for mutants E276Q and D393N, on the other.

Regarding the first pair of acidic residues, mutations of residues D274 and D395 do not affect similarly the fusion properties of the glycoprotein. However, mutants D274N and D395N are affected similarly in their pseudotyping efficiency compared to WT G. Furthermore, the fast reversion to the wild-type protein sequence in the reverse genetics experiments emphasizes the importance of these two residues.

If one considers now the second pair of acidic residues, whatever property is characterized, mutant E276Q cannot be distinguished from WT G, whereas mutant D393N is extremely affected in its fusion properties and its pseudotyping ability. Furthermore, although VSV G.E276Q has the same behavior as the WT VSV, mutant VSV G.D393N immediately reverted to the wild-type protein sequence in reverse genetics experiments. As a consequence, the residues E276 and D393, although facing each other in the postfusion state, do not form together a pH-sensitive molecular switch. It is therefore probable that the role of D393 is elsewhere, in the stabilization of a functional intermediate and/or some supramolecular assemblies.

Final remarks. In conclusion, this study provides experimental information on acidic residues that play the role of a pH-sensitive switch for the transition from the postfusion toward the prefusion state of VSV glycoprotein. It demonstrates that several residues are involved in this process. Although D268 appears to be a critical sensor, D274, D395, and D393 have additional contributions. The acidic character of the residues in positions 274, 395, and 393 is conserved among the *Vesiculovirus* genus, which is not the case for the residue found in position 268 (Fig. 10B). However, helices F and H of other vesiculovirus G proteins contain several acidic residues (Fig. 10B). Some of them may also be involved in the destabilization of the low-pH form above pH 7.

Globally, the situation is a bit more complex than for the flavivirus and alphavirus envelope fusion glycoproteins, for which single histidines have been identified to be the critical pH sensors involved in the transition from the pre- to the postfusion states (38, 39). Finally, this work also demonstrates the critical role of the fine-tuning of the stability of central helix F in this process. These new insights suggest that the segment consisting of residues 264 to 273, which refolds during the structural transition, might be a good target for antiviral compounds as any modification of its propensity to adopt a helical conformation is detrimental for the virus.

ACKNOWLEDGMENTS

We are very grateful to Aurélie Albertini, Frauje Beilstein, Danielle Blondel, Stéphane Bressanelli, Cécile Lagaudrière, and Stéphane Roche for helpful discussions throughout this project. We thank members of Peter Rottier's lab for the gift of the VSV pseudotype system.

This work was supported by the European Union through the Marie Curie ITN Project Virus Entry (reference 235649) (Ph.D. grants for E.B. and A.F.), a grant from Agence Nationale de la Recherche (ANR-11-BSV8-002) (postdoctoral grant for E.B.), and by the Fondation pour la Recherche Médicale (FRM DEQ20120323711).

REFERENCES

1. **Albertini A, Bressanelli S, Lepault J, Gaudin Y.** 2011. Structure and working of viral fusion machinery. Curr. Top. Membr. **68:**49–80. http://dx.doi.org/10.1016/B978-0-12-385891-7.00003-9.
2. **Harrison SC.** 2008. Viral membrane fusion. Nat. Struct. Mol. Biol. **15:**690–698. http://dx.doi.org/10.1038/nsmb.1456.
3. **Li Y, Modis Y.** 2014. A novel membrane fusion protein family in *Flaviviridae*? Trends Microbiol. **22:**176–182. http://dx.doi.org/10.1016/j.tim.2014.01.008.
4. **Gaudin Y.** 2000. Reversibility in fusion protein conformational changes. The intriguing case of rhabdovirus-induced membrane fusion. Subcell. Biochem. **34:**379–408. http://dx.doi.org/10.1007/0-306-46824-7_10.
5. **Anderson RG, Orci L.** 1988. A view of acidic intracellular compartments. J. Cell Biol. **106:**539–543. http://dx.doi.org/10.1083/jcb.106.3.539.
6. **Sugrue RJ, Bahadur G, Zambon MC, Hall-Smith M, Douglas AR, Hay AJ.** 1990. Specific structural alteration of the influenza haemagglutinin by amantadine. EMBO J. **9:**3469–3476.
7. **Pinto LH, Holsinger LJ, Lamb RA.** 1992. Influenza virus M2 protein has ion channel activity. Cell **69:**517–528. http://dx.doi.org/10.1016/0092-8674(92)90452-I.
8. **Stieneke-Grober A, Vey M, Angliker H, Shaw E, Thomas G, Roberts C, Klenk HD, Garten W.** 1992. Influenza virus hemagglutinin with multibasic cleavage site is activated by furin, a subtilisin-like endoprotease. EMBO J. **11:**2407–2414.
9. **Skehel JJ, Wiley DC.** 2000. Receptor binding and membrane fusion in virus entry: the influenza hemagglutinin. Annu. Rev. Biochem. **69:**531–569. http://dx.doi.org/10.1146/annurev.biochem.69.1.531.
10. **Heinz FX, Stiasny K, Puschner-Auer G, Holzmann H, Allison SL, Mandl CW, Kunz C.** 1994. Structural changes and functional control of the tick-borne encephalitis virus glycoprotein E by the heterodimeric association with protein prM. Virology **198:**109–117. http://dx.doi.org/10.1006/viro.1994.1013.
11. **Lobigs M, Garoff H.** 1990. Fusion function of the Semliki Forest virus spike is activated by proteolytic cleavage of the envelope glycoprotein precursor p62. J. Virol. **64:**1233–1240.
12. **Rose JK, Whitt MA.** 2001. *Rhabdoviridae*: the viruses and their replication, p 1221–1224. *In* Knipe DM, Howley PM, Griffin DE, Lamb RA, Martin MA, Roizman B, Straus SE (ed), Fields virology, 4th ed. Lippincott Williams & Wilkins, Philadelphia, PA.
13. **Albertini AAV, Baquero E, Ferlin A, Gaudin Y.** 2012. Molecular and cellular aspects of rhabdovirus entry. Viruses **4:**117–139. http://dx.doi.org/10.3390/v4010117.
14. **Doms RW, Keller DS, Helenius A, Balch WE.** 1987. Role for adenosine triphosphate in regulating the assembly and transport of vesicular stomatitis virus G protein trimers. J. Cell Biol. **105:**1957–1969. http://dx.doi.org/10.1083/jcb.105.5.1957.
15. **Gaudin Y, Ruigrok RW, Knossow M, Flamand A.** 1993. Low-pH conformational changes of rabies virus glycoprotein and their role in membrane fusion. J. Virol. **67:**1365–1372.
16. **Libersou S, Albertini AA, Ouldali M, Maury V, Maheu C, Raux H, de Haas F, Roche S, Gaudin Y, Lepault J.** 2010. Distinct structural rearrangements of the VSV glycoprotein drive membrane fusion. J. Cell Biol. **191:**199–210. http://dx.doi.org/10.1083/jcb.201006116.
17. **Albertini AA, Merigoux C, Libersou S, Madiona K, Bressanelli S, Roche S, Lepault J, Melki R, Vachette P, Gaudin Y.** 2012. Characterization of monomeric intermediates during VSV glycoprotein structural transition. PLoS Pathog. **8:**e1002556. http://dx.doi.org/10.1371/journal.ppat.1002556.
18. **Roche S, Gaudin Y.** 2002. Characterization of the equilibrium between the native and fusion-inactive conformation of rabies virus glycoprotein indicates that the fusion complex is made of several trimers. Virology **297:**128–135. http://dx.doi.org/10.1006/viro.2002.1429.
19. **Gaudin Y, Tuffereau C, Durrer P, Flamand A, Ruigrok RW.** 1995. Biological function of the low-pH, fusion-inactive conformation of rabies virus glycoprotein (G): G is transported in a fusion-inactive state-like conformation. J. Virol. **69:**5528–5534.
20. **Roche S, Rey FA, Gaudin Y, Bressanelli S.** 2007. Structure of the prefusion form of the vesicular stomatitis virus glycoprotein G. Science **315:**843–848. http://dx.doi.org/10.1126/science.1135710.
21. **Roche S, Bressanelli S, Rey FA, Gaudin Y.** 2006. Crystal structure of the low-pH form of the vesicular stomatitis virus glycoprotein G. Science **313:**187–191. http://dx.doi.org/10.1126/science.1127683.
22. **Sun X, Belouzard S, Whittaker GR.** 2008. Molecular architecture of the bipartite fusion loops of vesicular stomatitis virus glycoprotein G, a class III viral fusion protein. J. Biol. Chem. **283:**6418–6427. http://dx.doi.org/10.1074/jbc.M708955200.
23. **Stanifer ML, Cureton DK, Whelan SP.** 2011. A recombinant vesicular

stomatitis virus bearing a lethal mutation in the glycoprotein gene uncovers a second site suppressor that restores fusion. J. Virol. **85:**8105–8115. http://dx.doi.org/10.1128/JVI.00735-11.

24. **Baquero E, Albertini AA, Vachette P, Lepault J, Bressanelli S, Gaudin Y.** 2013. Intermediate conformations during viral fusion glycoprotein structural transition. Curr. Opin. Virol. **3:**143–150. http://dx.doi.org/10.1016/j.coviro.2013.03.006.
25. **Pasdeloup D, Poisson N, Raux H, Gaudin Y, Ruigrok RW, Blondel D.** 2005. Nucleocytoplasmic shuttling of the rabies virus P protein requires a nuclear localization signal and a CRM1-dependent nuclear export signal. Virology **334:**284–293. http://dx.doi.org/10.1016/j.virol.2005.02.005.
26. **Matsuura Y, Tani H, Suzuki K, Kimura-Someya T, Suzuki R, Aizaki H, Ishii K, Moriishi K, Robison CS, Whitt MA, Miyamura T.** 2001. Characterization of pseudotype VSV possessing HCV envelope proteins. Virology **286:**263–275. http://dx.doi.org/10.1006/viro.2001.0971.
27. **Tani H, Komoda Y, Matsuo E, Suzuki K, Hamamoto I, Yamashita T, Moriishi K, Fujiyama K, Kanto T, Hayashi N, Owsianka A, Patel AH, Whitt MA, Matsuura Y.** 2007. Replication-competent recombinant vesicular stomatitis virus encoding hepatitis C virus envelope proteins. J. Virol. **81:**8601–8612. http://dx.doi.org/10.1128/JVI.00608-07.
28. **Lawson ND, Stillman EA, Whitt MA, Rose JK.** 1995. Recombinant vesicular stomatitis viruses from DNA. Proc. Natl. Acad. Sci. U. S. A. **92:**4477–4481. http://dx.doi.org/10.1073/pnas.92.10.4477.
29. **Schnell MJ, Buonocore L, Whitt MA, Rose JK.** 1996. The minimal conserved transcription stop-start signal promotes stable expression of a foreign gene in vesicular stomatitis virus. J. Virol. **70:**2318–2323.
30. **Hammond C, Helenius A.** 1995. Quality control in the secretory pathway. Curr. Opin. Cell Biol. **7:**523–529. http://dx.doi.org/10.1016/0955-0674(95)80009-3.
31. **Dunphy WG, Rothman JE.** 1985. Compartmental organization of the Golgi stack. Cell **42:**13–21. http://dx.doi.org/10.1016/S0092-8674(85)80097-0.
32. **Desmezieres E, Maillard AP, Gaudin Y, Tordo N, Perrin P.** 2003. Differential stability and fusion activity of lyssavirus glycoprotein trimers. Virus Res. **91:**181–187. http://dx.doi.org/10.1016/S0168-1702(02)00267-8.
33. **Jeetendra E, Ghosh K, Odell D, Li J, Ghosh HP, Whitt MA.** 2003. The membrane-proximal region of vesicular stomatitis virus glycoprotein G ectodomain is critical for fusion and virus infectivity. J. Virol. **77:**12807–12818. http://dx.doi.org/10.1128/JVI.77.23.12807-12818.2003.
34. **Nakai T, Howatson AF.** 1968. The fine structure of vesicular stomatitis virus. Virology **35:**268–281. http://dx.doi.org/10.1016/0042-6822(68)90267-5.
35. **Brown JC, Newcomb WW, Lawrenz-Smith S.** 1988. pH-dependent accumulation of the vesicular stomatitis virus glycoprotein at the ends of intact virions. Virology **167:**625–629. http://dx.doi.org/10.1016/0042-6822(88)90126-2.
36. **Barge A, Gaudin Y, Coulon P, Ruigrok RW.** 1993. Vesicular stomatitis virus M protein may be inside the ribonucleocapsid coil. J. Virol. **67:**7246–7253.
37. **Roche S, Albertini AA, Lepault J, Bressanelli S, Gaudin Y.** 2008. Structures of vesicular stomatitis virus glycoprotein: membrane fusion revisited. Cell. Mol. Life Sci. **65:**1716–1728. http://dx.doi.org/10.1007/s00018-008-7534-3.
38. **Qin ZL, Zheng Y, Kielian M.** 2009. Role of conserved histidine residues in the low-pH dependence of the Semliki Forest virus fusion protein. J. Virol. **83:**4670–4677. http://dx.doi.org/10.1128/JVI.02646-08.
39. **Fritz R, Stiasny K, Heinz FX.** 2008. Identification of specific histidines as pH sensors in flavivirus membrane fusion. J. Cell Biol. **183:**353–361. http://dx.doi.org/10.1083/jcb.200806081.
40. **Obiang L, Raux H, Ouldali M, Blondel D, Gaudin Y.** 2012. Phenotypes of vesicular stomatitis virus mutants with mutations in the PSAP motif of the matrix protein. J. Gen. Virol. **93:**857–865. http://dx.doi.org/10.1099/vir.0.039800-0.
41. **Grigorov B, Rabilloud J, Lawrence P, Gerlier D.** 2011. Rapid titration of measles and other viruses: optimization with determination of replication cycle length. PLoS One **6:**e24135. http://dx.doi.org/10.1371/journal.pone.0024135.